

Kinetics of Heterogeneous Electron Transfer at Liquid/Liquid Interfaces As Studied by SECM

Zhifeng Ding, Bernadette M. Quinn, and Allen J. Bard*

Department of Chemistry and Biochemistry, The University of Texas at Austin, Austin, Texas 78712

Received: January 7, 2001; In Final Form: May 1, 2001

Scanning electrochemical microscopy (SECM) was used to investigate the kinetics of heterogeneous electron transfer (ET) as a function of driving force at the interface between two immiscible electrolyte solutions. At high driving force, experimental rate constants decreased with increasing overpotential, deviating from predictions based on Butler–Volmer kinetics. This decrease in ET rate with increasing driving force is consistent with Marcus theory inverted region behavior. At low driving force, the potential dependence of the forward and reverse ET rate constants followed Butler–Volmer theory. SECM is also demonstrated to be a useful means of studying the effect of high ionic strength on the kinetics of heterogeneous ET.

Introduction

There is renewed interest in heterogeneous electron transfer (ET) reactions at the interface between two immiscible electrolyte solutions (ITIES). The application of new techniques such as scanning electrochemical microscopy (SECM),^{1–3} microelectrochemical measurements at expanding droplets (MIMED),^{4,5} thin-layer cyclic voltammetry (CV),^{6–8} and spectroelectrochemical methods⁹ has greatly increased the amount of kinetic data available. These studies are considered to be a very useful means of testing conventional theories for ET kinetics.^{2,9,10} In this report, SECM was used to verify the existence of the Marcus inverted region^{11–13} at high driving force.

Heterogeneous ET at a liquid/liquid interface involves the transfer of an electron under potential control from an electron donor to an acceptor in opposing phases. In earlier studies,^{14,15} the interface was under potentiostatic control, and the finite potential window, governed by ion transfer processes, limited the number of redox reactions that could be studied and hindered experimental studies. The residual uncompensated solution resistance due to the low permittivity of organic solvents ($\epsilon < 10$) used and the high double-layer capacitance also made reliable kinetic data difficult to obtain. SECM has been demonstrated to overcome these restrictions.^{2,16,17} As the interface is nonpolarized and the heterogeneous ET is followed by feedback to an SECM tip, the number of solvent systems and redox couples that can be used greatly increased. For example, benzene could not be used as the organic solvent in conventional systems without the addition of very large amounts of base electrolyte, which would in turn severely limit the size of the available potential window.

Previous studies with SECM allowed reliable kinetic data at liquid/liquid interfaces to be obtained, and at low overpotentials, the kinetics of ET appear to follow Butler–Volmer (B–V) theory.¹⁷ As the driving force is increased, Marcus theory predicts the existence of an inverted region where the rate decreases with increasing driving force.^{12,13} Probing the existence of such an inverted region is difficult with conventional electrochemical techniques. As the SECM technique does not suffer from potential window restrictions, the driving force can be increased readily by the appropriate choice of redox couples

and potential determining ions. However, with these initial SECM studies, with high concentrations of reactant in the aqueous phase, the rates at high driving forces became limited by diffusion, and the actual ET rate constants could not be extracted. Tsionsky et al.¹⁷ demonstrated the existence of an inverted region in the presence of an interfacial phospholipid monolayer. The monolayer served to increase the distance between reaction centers, and the rate constant was decreased below the diffusion limit. Electrogenerated chemiluminescence (ECL) combined with SECM studies by Zu et al.¹⁸ also suggested the existence of an inverted region at an unmodified interface. In these earlier studies, one redox couple was added in excess and heterogeneous ET was treated as a pseudo-first-order reaction to simplify the diffusion problem. However, for fast kinetics, diffusion is rate limiting, and this sets an upper limit for the accessible experimental rate constant.¹⁷ Recently, this limit was greatly increased by Barker et al.² by employing a model in which diffusion of both reactants in opposing phases was considered. Depending on the concentration ratios of reactants employed, the authors suggest that rate constants in excess of $500 \text{ cm s}^{-1} \text{ M}^{-1}$ are accessible to experimental determination. Experimental results presented in this work also suggested the existence of an inverted region at the unmodified liquid/liquid interface. However, the number of redox couples studied was small, so the conclusion about inverted region behavior was somewhat ambiguous. Here, this work is extended for the heterogeneous ET between organic phase tetraphenylzinc porphyrin (ZnPor) and a variety of aqueous redox couples at three different water/organic solvent systems.

Another aspect of the studies of ET at the ITIES concerns the potential dependence of the rate constant. It is assumed in both B–V and Marcus theories that most of the interfacial potential drop is between the reaction centers and that the potential dependence of the rate constant can be directly related to the free energy of ET.¹⁷ Recently, this assumption has been questioned, and the observed potential dependence of the rate constant was attributed to a double-layer effect due to the potential controlled variation of the charged redox reactant concentrations in the interfacial region.¹⁹ Liu and Mirkin¹⁰ considered this possibility for ET involving a neutral reactant and noted that the experimental ET rate constant was essentially

potential independent. A similar approach was used here to probe the potential dependence of the forward and reverse rate constants for ET involving neutral organic phase tetracyanoquinodimethane (TCNQ) and aqueous hexacyanoferrate. The driving force for this ET is low, and the forward and reverse reactions can be easily studied by the appropriate choice of potential determining ion.

The ionic strength of both phases also affects the potential distribution across the interface. This can have a significant effect on experimental kinetic parameters,^{20,21} for example, the Frumkin effect at metallic electrodes. SECM offers a convenient means of monitoring the effect of increasing ionic strength on ET kinetics.

Experimental Section

Chemicals. Tetrahexylammonium perchlorate (THxAClO₄) (Fluka) was recrystallized from acetone prior to use. Tetrahexylammonium hexafluorophosphate (THxAPF₆), tetracyanoquinodimethane (TCNQ) (Aldrich), 5,10,15,20-tetraphenyl 21*H*,23*H*-porphyrin zinc (ZnPor) (Aldrich), NaCl, NaClO₄, Na₄Fe(CN)₆, VCl₃, and cobalt sepulchrate chloride (Co(Sep)³⁺) were used without further purification. The organic solvents chosen for study, 1,2-dichloroethane (1,2-DCE) (Aldrich), benzonitrile (BN) (Sigma), and benzene (Aldrich) were used as received.

Organic solutions were generally prepared with 0.25 M THxAClO₄ or prepared as indicated in the text. Aqueous solutions with varying concentrations of redox species were generally prepared with 0.1 M NaCl and 0.1 M NaClO₄. For measurements with V²⁺, NaCl was replaced with 0.5 M HCl. Na₄Ru(CN)₆, Na₄Mo(CN)₆, and FeEDTA²⁻ were prepared as previously described.² V²⁺ and Co(Sep)²⁺ solutions were prepared in a N₂-filled glovebag (Aldrich) prior to measurement by reduction of solutions of V³⁺ or Co(Sep)³⁺ with freshly prepared zinc amalgam.²² All aqueous solutions were prepared with MilliQ water.

Electrochemical Cells. SECM tips were prepared by heat-sealing Pt wires (25 μm diameter, Goodfellow, U.K.) in borosilicate glass capillaries under vacuum, followed by polishing and sharpening as previously described.²³ The viability of the resulting tip was determined by slow sweep CV in a 2 mM ferrocyanide +0.1 M KCl solution. Tips were characterized by an RG ($=r_g/a$, where r_g is the tip radius and a the radius of the Pt wire) between 3 and 4 as shown in Figure 1. The tip was rinsed with water and ethanol and dried prior to each measurement. A simplified two-electrode arrangement was used throughout, where a conventional reference electrode served as the counter and reference electrode. The reference electrodes, Ag/AgCl, Ag/AgClO₄, and Ag/AgPF₆, were prepared by electrodepositing AgCl, AgClO₄, and AgPF₆ onto an Ag wire, respectively. Electrodes were placed in the upper phase for all measurements as illustrated in Figure 2. For measurements at the water/DCE interface, a modified cell²⁴ was used to enable the higher density DCE to be used as the upper phase (Figure 2b). SECM experiments with air-sensitive redox species (FeEDTA²⁻, V²⁺, Co(Sep)²⁺) were performed under nitrogen in a glovebag (Aldrich).

SECM Setup. The SECM setup has been described in detail elsewhere.²³ Briefly, the tip was placed in the upper phase, and a cyclic voltammogram was recorded for the redox species used. Subsequently, the tip was biased at a potential in the diffusion-limited region. Approach curves, where tip current is monitored as a function of distance, d , were obtained by moving the tip toward the interface. The tip current was normalized by the diffusion limiting current $i_{T,\infty}$ ($=4nFDCa$ where D represents

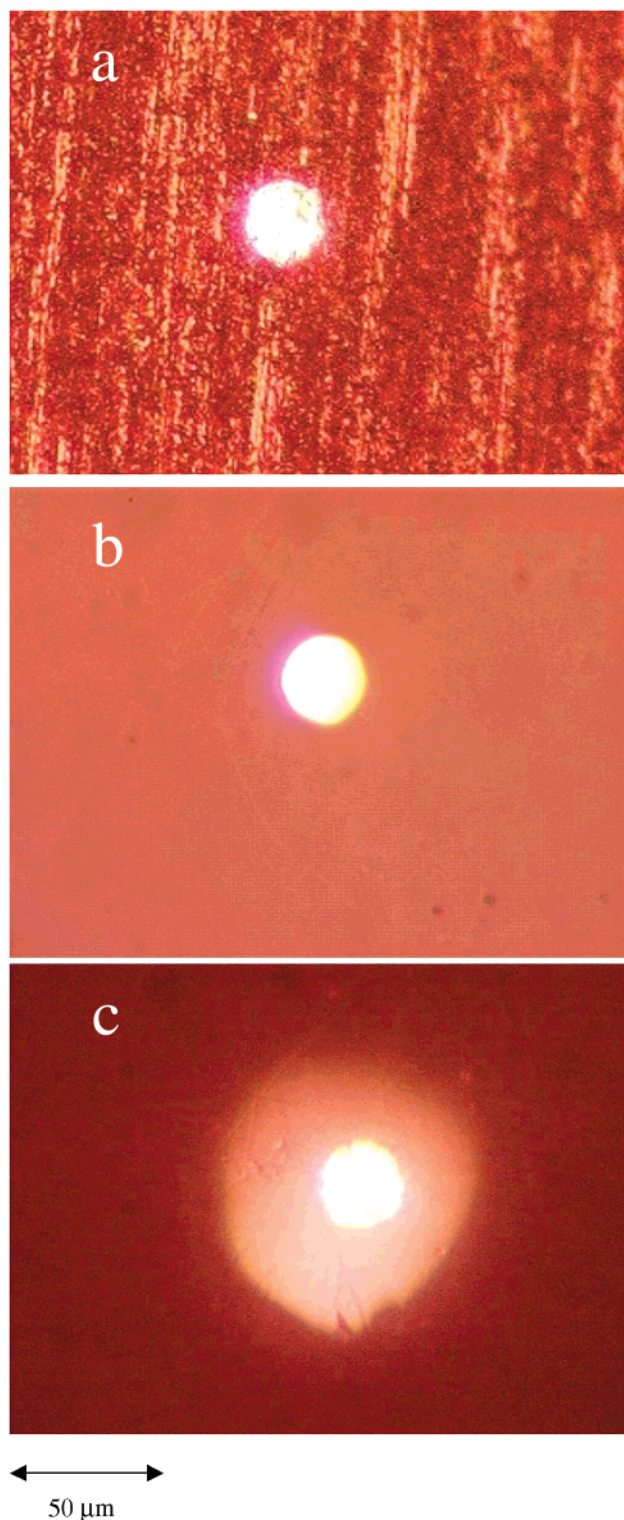


Figure 1. Video micrographs illustrating the steps involved in tip preparation: (a) unpolished microelectrode with $RG \gg 10$; (b) after polishing with alumina; and (c) after sharpening to $RG \approx 3-4$.

the diffusion coefficient and C the bulk concentration of the redox couple, a is the electrode radius, and F is Faraday's constant). All approach curves were obtained in the feedback mode.

Theoretical Section

Driving Force Dependence of Heterogeneous ET Rate at the ITIES.¹ The dependence of the second-order ET rate

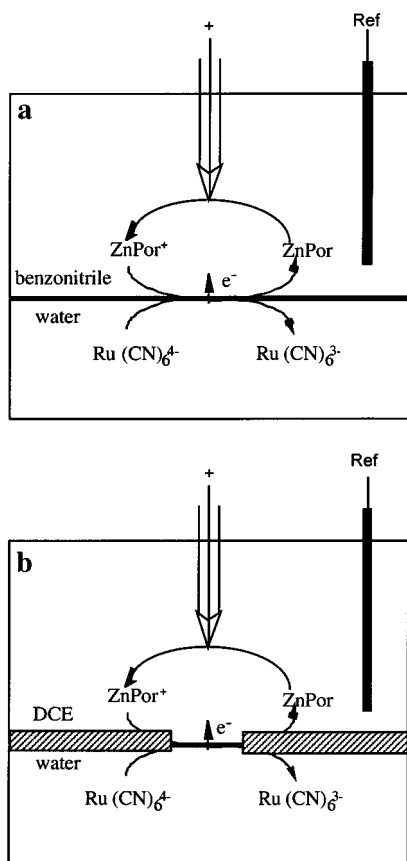


Figure 2. Schematics of SECM cells used to investigate ET at the liquid/liquid interface with (a) less dense phase on top and (b) modified cell with annulus to support the more dense phase on top. Ref denotes a reference electrode that served as both reference and counter electrode. The reference electrode was Ag/AgCl, Ag/AgClO₄, or Ag/AgPF₆ (see Experimental Section).

constant, k_{12} , on the energy of activation, ΔG^\ddagger , is given by

$$k_{12} = \text{const} \exp(-\Delta G^\ddagger/RT) \quad (1)$$

At lower overpotentials, a Butler–Volmer type approximation is applicable:¹

$$\Delta G^\ddagger = \alpha F(\Delta E^\circ + \Delta_w^\circ \phi) \quad (2)$$

where ΔE° is the difference between the standard potentials of two redox couples in opposing phases, $\Delta_w^\circ \phi$ is the Galvani potential difference, and α is the transfer coefficient. In the presence of a common ion, i , in both phases, the Galvani potential difference across the interface is determined by a Nernst type equation:²⁵

$$\Delta_w^\circ \phi = \Delta_w^\circ \phi^{\circ'} + (RT/z_i F) \ln(C_i^w/C_i^o) \quad (3)$$

where $\Delta_w^\circ \phi^{\circ'}$ and z_i represent the formal transfer potential and the charge of the partitioning ion, respectively. When the overpotential is high, in the absence of work terms, the energy of activation for an ET reaction is given by Marcus theory²⁶

$$\Delta G^\ddagger = \left(\frac{\lambda}{4}\right) \left(1 + \frac{\Delta G^\circ}{\lambda}\right)^2 \quad (4)$$

where λ is the reorganization energy, and ΔG° is given by¹

$$\Delta G^\circ = -F(\Delta E^\circ + \Delta_w^\circ \phi) \quad (5a)$$

According to eq 4, the activation energy of the ET reaction depends parabolically on ΔG° and, in the Marcus inverted region at large ΔG° values, increases as the driving force increases.

The ET rate constant depends, therefore, on the two types of driving forces, the $\Delta_w^\circ \phi$ term and the difference in standard potentials of the organic and aqueous redox mediators, ΔE° , as shown in eq 5a. These were investigated by changing the above two parameters.

The formal potentials of the aqueous ($E_{O_1/R_1}^{0,w}$) and organic ($E_{O_2/R_2}^{0,o}$) redox couples were taken as the half wave potentials obtained from ultramicroelectrode cyclic voltammograms by the same technique as reported previously.¹⁷ The difference in formal potentials for the aqueous and organic redox species ($\Delta E_{1/2}$) versus the same reference electrode gives the absolute value of the driving force for the ET:^{3,17}

$$\Delta E_{1/2} = \Delta E^\circ + \Delta_w^\circ \phi \quad (5b)$$

where $\Delta E^\circ = E_{O_1/R_1}^{0,w} - E_{O_2/R_2}^{0,o}$ versus the same reference electrode and $\Delta_w^\circ \phi$ is as given by eq 3. Thus, the driving force can be changed by a suitable choice of the redox couples or the potential determining ions. To verify Marcus theory, the driving force must be increased over a wide potential range, and in this case, this was achieved by varying the aqueous redox couple. At low driving force, the potential dependence of the forward and reverse rate constants was followed through variation of the potential determining ion.

SECM Curve Fitting. The concentration ratio K_r of aqueous to organic reductant ($K_r = C_{R_2}^{*,w}/C_R^{*,o}$) determines the upper limit for the accessible rate constant.² For $K_r > 20$, the aqueous reductant is in excess, and the reaction can be treated as pseudo-first-order. This is useful when the rate of ET is slow and the analytical approximation eq 6b in ref 16 can be used to determine the rate constant. For lower values of K_r , diffusion of both redox couples needs to be considered, and the procedure proposed by Barker et al.² was adopted to extract the rate constant. This involved comparison of experimental approach curves with families of simulated approach curves as a function of rate constant for each K_r . By using a small value of K_r , mass transfer limits on the experimental accessibility of the rate constant can be overcome. This more general theory also enables one to identify the K_r range where the constant composition approximation is valid. Furthermore, the use of relatively low concentrations of the reactant in the second phase was theoretically predicted to have considerable advantages for lowering the ET reaction rate and causing the approach curves in the fast kinetic limit to be more readily distinguished from one another.

Experimental approach curves for several K_r values were fit to simulated curves to obtain the rate constant for each aqueous redox couple used. Program input parameters were as follows: the diffusion coefficients and concentration of the two reactants, the rate constant, the diameter of the ultramicroelectrode, and the tip RG value. A FORTRAN program generously provided by Prof. P. R. Unwin was used to simulate the theoretical approach curves. The program was written for an SECM tip with an RG = 10, while the experimental tips were considerably smaller (3.5 to 4). The reason for using a tip with such a small RG was to avoid contacting the interface with the tip glass sheath. This enabled us to approach the interface more closely than with a larger RG tip. Shao and Mirkin²⁷ demonstrated that as RG \rightarrow 1, negative feedback is less efficient, and the SECM approach curve to an insulator deviates from theory for RG \gg 1. The possible error introduced by this difference was tested

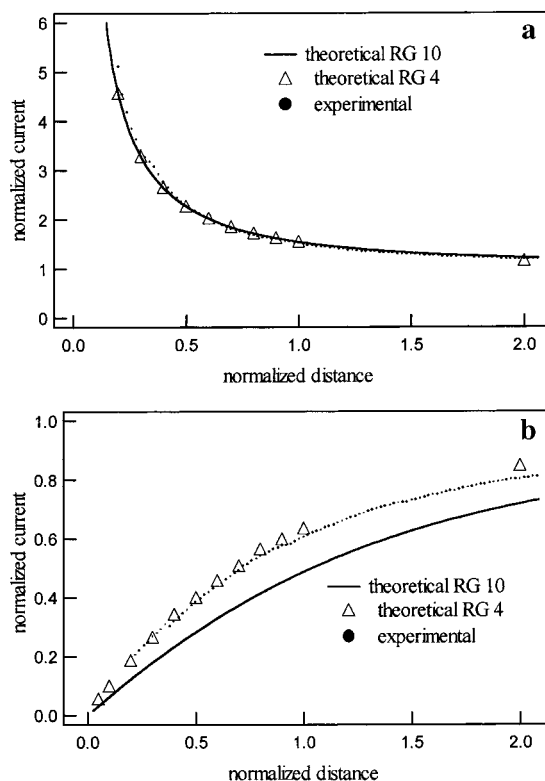
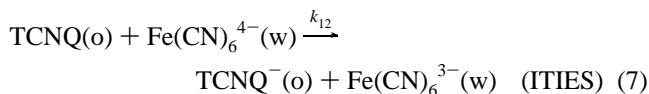
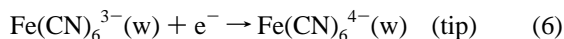


Figure 3. Comparison of simulated normalized steady-state current SECM approach curves to (a) an insulating substrate and (b) a conducting substrate for tip RG = 10 (—) and 4 (Δ) and for the experimental tip used (\bullet). Experimental curves were obtained with an aqueous solution of 2 mM $\text{Na}_4\text{Fe}(\text{CN})_6$ and 0.1 M NaCl. Current was normalized by infinite current $i_{T,\infty} = 6.20$ nA.

by solving the diffusion problem with PDEase²⁸ and generating approach curves as a function of RG . However, as can be seen from Figure 3, theoretical approach curves for $RG = 10$ and 4 and the experimental one for our tip are practically coincident at the conductor interface. And, those at the insulating substrate are considered to be within reasonable experimental error. Thus, the fitting program was used without modification.

Results and Discussion

1. Dependence of the ET Rate on the Galvani Potential Difference at the ITIES—Butler–Volmer Behavior. SECM approach curves were obtained to study the ET reaction between $\text{Fe}(\text{CN})_6^{4-}$ in water (w) and TCNQ in DCE (o), that is



In these experiments $C_{\text{ClO}_4^-}^0$ was maintained constant and, from eq 3, $\Delta^0_w \phi$ shifts by 59 mV to more negative values with each decade increase in $C_{\text{ClO}_4^-}^w$. The driving force for eq 7 is low ($\Delta E_{1/2} \approx 5$ to -80 mV under the given experimental conditions), and a linear driving force dependence of activation energy is expected. Approach curves for a range of K_r were fit by the models developed by Wei et al. ($K_r = 20$)¹⁶ and Barker et al. ($K_r < 20$)² to extract the second-order rate constant. In the latter case, three-to-four ratios were generally used ($0.1 < K_r < 10$), and the bimolecular rate constant for each ratio, obtained from the fitting program, agreed within experimental error as reported

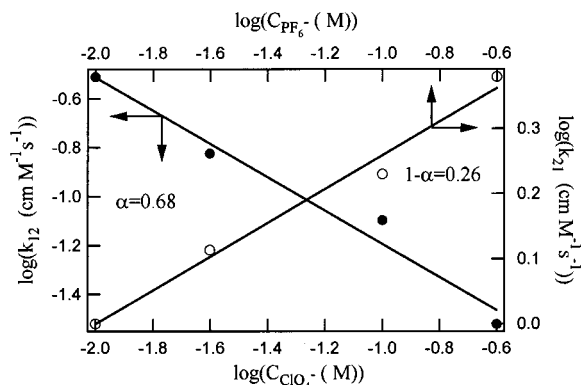


Figure 4. Tafel plots illustrating the potential dependence of the forward k_{12} and reverse k_{21} rate constants for ET between aqueous hexacyanoferrate and organic phase TCNQ at the DCE/water interface. The interfacial potential difference was varied through the potential determining ions chosen (ClO_4^- or PF_6^-) and the aqueous to organic concentration ratio used. The concentrations of TCNQ and $\text{Fe}(\text{CN})_6^{3-}$ for measurements of k_{12} (reaction 7) were 5 and 2 mM respectively, and the concentrations of TCNQ and $\text{Fe}(\text{CN})_6^{4-}$ for measurements of k_{21} were 1 and 20 mM, respectively.

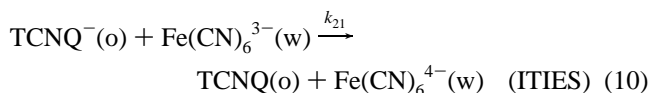
previously. Measurements at $K_r < 20$ have the additional advantage of overcoming the uncertainty in determining the absolute tip distance from the interface. As predicted theoretically and noted experimentally here, approach curves at lower K_r have a distinctive shape, with the appearance of a peak when the tip is close to the interface. Such curves are more convenient for fitting, and therefore uncertainties in d become smaller.

From eqs 1–3, the following relation is obtained (with a constant composition of the DCE phase):

$$\log k_{12} = \text{const} - \alpha \log C_{\text{ClO}_4^-}^w \quad (8)$$

A Tafel type plot, that is, $\log k_{12}$ versus $\log C_{\text{ClO}_4^-}^w$, is given in Figure 4. As $C_{\text{ClO}_4^-}^w$ increases, corresponding to a less positive $\Delta^0_w \phi$ value, $\log k_{12}$ decreases linearly with decreasing $\Delta^0_w \phi$. The transfer coefficient obtained from the slope was 0.68 ± 0.1 for 2 mM $\text{Fe}(\text{CN})_6^{3-}$ in aqueous solution and in a solution of 5 mM TCNQ in DCE. This is consistent with predictions based on eq 2 and suggests that Butler–Volmer kinetics can be used to describe this ET when the driving force is low. The α could differ in principle from 0.5, a common value in metal–liquid systems, because of the work terms which are due to double-layer effects in both phases and to the interaction of reactants.¹² A similar result was obtained by Unwin et al.²⁰ However, it has been suggested that this is not necessarily a confirmation of B–V theory, as concentration changes of the reacting species with the electric field at the interface would induce a similar potential dependence.^{10,19} This is discussed in more detail in the next section.

To fully verify the applicability of B–V theory, the kinetics of the back reaction of eq 7, that is, TCNQ in DCE (o) and $\text{Fe}(\text{CN})_6^{3-}$ in water (w), were also studied:



In this case, PF_6^- was used as the partitioning ion because of its suitable transfer potential ($\Delta^0_w \phi^{\circ'} = 43\text{mV}$)²⁹ which is less positive than that for ClO_4^- ($\Delta^0_w \phi^{\circ'} = 170$ mV), and therefore

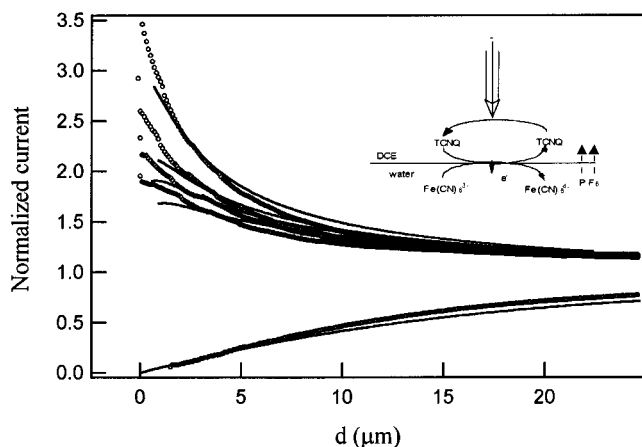


Figure 5. Experimental SECM approach curves for the reverse ET reaction between aqueous $\text{Fe}(\text{CN})_6^{3-}$ and tip generated organic phase TCNQ⁻ for different $[\text{PF}_6^-]_{\text{aq}} = 0.25, 0.1, 0.025,$ and 0.01 M (top to bottom). Current was normalized with $i_{T,\infty} = 3.20$ nA, and 0.1 M NaCl was added to the aqueous solution to keep the ionic strength essentially constant. $[\text{PF}_6^-]_{\text{DCE}} = 0.01$ M and a reactant concentration ratio $K_r = 20$ were used throughout. The concentrations of TCNQ and $\text{Fe}(\text{CN})_6^{3-}$ were 1 and 20 mM, respectively. Solid lines represent the theory for the rate constant obtained through fitting for each $[\text{PF}_6^-]_{\text{aq}}$. An example of an approach curve to an insulating liquid/liquid interface ($[\text{Fe}(\text{CN})_6^{3-}] = 0$ M) is also given for comparison.

reaction 10 is easier to drive by using PF_6^- than using ClO_4^- . Similar reverse uphill ET reactions at a liquid/liquid interface have already been illustrated by changing the partitioning ion as in our previous report.³⁰ The driving force was varied by increasing $C_{\text{PF}_6^-}^w$ at constant $C_{\text{PF}_6^-}^o$ (eq 3). Analogously to eq 8, we can write the B–V equation for eq 10:

$$\log k_{21} = \text{const} + \beta \log C_{\text{PF}_6^-}^w \quad (11)$$

Typical approach curves of the SECM measurements are shown in Figure 5 for various PF_6^- concentrations in aqueous solution while that in DCE was kept constant (10 mM), and curves were fit as described above to obtain the rate constant. The concentrations for TCNQ and $\text{Fe}(\text{CN})_6^{4-}$ are 1 and 20 mM, respectively. The resulting plot of $\log k_{21}$ versus $\log C_{\text{PF}_6^-}^w$ is given in Figure 4, and as expected, $\log k_{21}$ increases linearly with decreasing $\Delta^o_w \phi$. The ET transfer coefficient obtained from the slope, β , is 0.26 . Thus, $\alpha + \beta \approx 1$, as expected for a reaction following B–V kinetics.³¹

Previously, the suitability of this system was questioned,¹⁰ as experimental data obtained did not fit theory. However, the organic base electrolyte anion used in that study, tetraphenylborate (TPB^-), can reduce TCNQ, and an analysis based on a CE mechanism is required.³¹ Girault and Schiffrin³² noted that the observed potential dependence of the rate constant could also be simply due to control of the reactant surface concentrations through the applied potential. Schmickler¹⁹ developed this idea and proposed an interfacial model where most of the potential drop is dissipated in the double layer, and a change of the potential difference between the two bulk phases will only slightly affect the driving force for an electron transfer reaction; however, it will change the concentration of ionic reactants at the interface. Thus, the rate constant is effectively potential independent for neutral species. As TCNQ is neutral, this model predicts a potential independent rate for reaction 7, assuming that most of the potential drop occurs in the organic phase. Liu and Mirkin¹⁰ presented results that support this concept with the ZnPor/hexacyanoferrate(II) system. However, for the TCNQ/

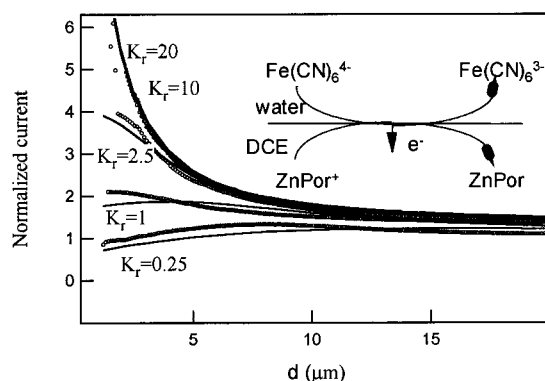


Figure 6. Experimental SECM approach curves for the heterogeneous ET reaction between aqueous $\text{Fe}(\text{CN})_6^{4-}$ and tip generated organic phase ZnPor^+ at the DCE/water interface for various reactant concentration ratios $K_r = 20, 10, 2.5, 1,$ and 0.25 (top to bottom). Current was normalized with $i_{T,\infty} = 1.90$ nA. Solid lines show the simulated curves for a bimolecular rate constant of $110 \text{ cm s}^{-1} \text{ M}^{-1}$.

hexacyanoferrate system presented here, the forward and reverse rate constants are clearly both potential dependent, indicating that, for this system, it is possible to vary the reaction free energy through the interfacial potential. From the results shown above, we conclude that reactions 7 and 10 are good systems for studying the potential dependence, as the potential difference, ΔE^o , between redox couples is small and the reaction direction, forward and backward, can be easily alternated.

2. Marcus Inverted Region at Unmodified ITIES. SECM measurement of rapid ET kinetics at unmodified ITIES is desirable for a better understanding of these processes. As reported previously,¹⁷ the rate constant for ET reactions with high driving forces for $K_r > 20$ could only be experimentally determined when an adsorbed surfactant was used as a spacer to increase the separation distance between the reactants.¹⁷ In the absence of this spacer, under the constant composition approximation used, the reaction was diffusion-limited, and the rate constant was given as a lower limit. However, as demonstrated by Barker et al.,² when K_r is decreased, the interfacial ET rate decreases, making larger rate constants accessible before diffusion limitations come into play.²

In this case, the redox reactions at the tip and ITIES are as follows



where the redox couple R/O represents $\text{Ru}(\text{CN})_6^{3-/4-}$, $\text{Mo}(\text{CN})_8^{3-/4-}$, $\text{Fe}(\text{CN})_6^{3-/4-}$, $\text{W}(\text{CN})_8^{3-/4-}$, $\text{Fe}(\text{EDTA})^{-2-}$, $\text{Ru}(\text{NH}_3)_6^{3+/2+}$, $\text{Co}(\text{Sep})^{3+/2+}$, and $\text{V}^{3+/2+}$. Here, the driving force increased by over 1.3 V by varying the aqueous reductant from hexacyanoruthenium to vanadium chloride or cobalt(II) sepulchrate, $\text{Co}(\text{Sep})^{2+}$, while the concentrations of the potential determining ion (ClO_4^-) in the two phases remained constant.

A set of normalized approach curves for ET between ZnPor^+ and $\text{Fe}(\text{CN})_6^{4-}$ (eq 13) at the DCE/water interface is given in Figure 6 for various K_r . As discussed in the previous section, the bimolecular rate constant for each ratio was obtained through fitting to the models developed by Wei et al. ($K_r = 20$)¹⁶ and Barker et al. ($K_r < 20$)² for $D_{\text{ZnPor}}^o = 2.5 \times 10^{-6} \text{ cm}^2 \text{ s}^{-1}$ and $D_{\text{Fe}(\text{CN})_6^{4-}}^w = 6.7 \times 10^{-6} \text{ cm}^2 \text{ s}^{-1}$.

As can be seen from this figure, the rate constant cannot be extracted (curve 1) for $K_r > 20$ with either model. As the driving force, $\Delta E_{1/2} = 585$, is large, the ET rate is too fast to be measured under these experimental conditions, as has been noted

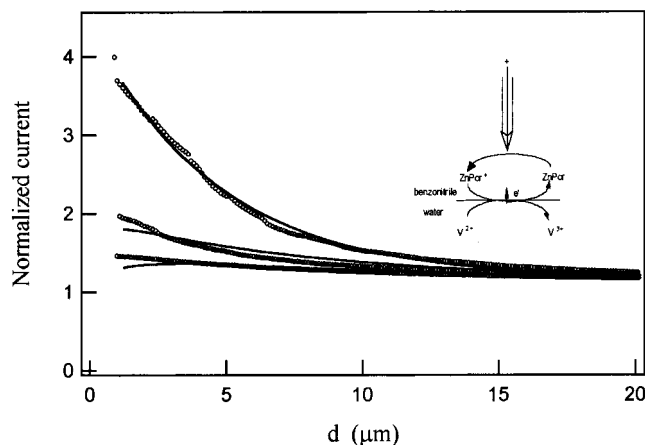


Figure 7. As in Figure 6 for the ET reaction between aqueous V^{2+} and tip generated organic phase $ZnPor^+$ at the BN/water interface where $K_r = 16, 4,$ and 2 (top to bottom). Current was normalized with $i_{T,\infty} = 2.30$ nA. Solid lines show the simulated curves for a bimolecular rate constant of 1.8 $cm\ s^{-1}\ M^{-1}$.

previously.¹⁷ For the lowest three approach curves, $K_r < 20$, the ET rate can be readily obtained, because decreasing the reactant concentrations decreases the ET rate. Best fits to the experimental data for a unique constant, $k_{12} = 110$ $cm\ s^{-1}\ M^{-1}$, are also given in Figure 6.

This reaction was also investigated at the benzene/water and BN/water interfaces (approach curves not shown), and the rate constants obtained were 80 and 85 $cm\ s^{-1}\ M^{-1}$. The latter value compares well with a previous report ($k_{12} = 91$ $cm\ s^{-1}\ M^{-1}$).²

Similarly, rate constants for the ET between $ZnPor^+/Ru(CN)_6^{4-}$ and $ZnPor^+/Mo(CN)_8^{4-}$ at the DCE/water interface were extracted. Values obtained were 2.5 and 15 $cm\ s^{-1}\ M^{-1}$, respectively, for given diffusion coefficients for $D_{Mo(CN)_8^{4-}}^w = 7.2 \times 10^{-6}$ $cm^2\ s^{-1}$. In these cases, the driving force is low with $\Delta E_{1/2} = 70$ mV in the former case and $\Delta E_{1/2} = 190$ mV in the latter. The rate increases with driving force, consistent with ET reactions in the normal Marcus region.

For the ET reaction between $ZnPor^+$ and V^{2+} at the BN/water interface, the driving force is high, $\Delta E_{1/2} \approx 1.3$ V. As before, experimental data were compared with simulated data as illustrated in Figure 7 to obtain the rate constant. The value obtained ($k_{12} = 2.8$ $cm\ s^{-1}\ M^{-1}$) is comparable to that obtained for $Ru(CN)_6^{4-}$ and is more than an order of magnitude lower than that obtained for $Fe(CN)_6^{4-}$. Thus, the rate decreased with increasing driving force, that is, Marcus inverted region ET was indicated. A similar trend was noted for ET between $ZnPor^+$ and $Co(Sep)^{2+}$ at the DCE/water interface. Although the driving force is more than 700 mV more positive than that for the $ZnPor^+/Fe(CN)_6^{4-}$ system, the k_{12} obtained from fitting the approach curves (Figure 8) was also more than an order of magnitude less (4 compared with 110 $cm\ s^{-1}\ M^{-1}$).

Rate constants for ET between $ZnPor^+$ and other aqueous reductants ($W(CN)_8^{4-}$, $Fe(EDTA)^{2-}$, $Ru(NH_3)_6^{2+}$) at the BN/water and benzene/water interfaces were obtained in a similar manner, and the driving force dependence of the bimolecular rate constant is given in Figure 9, where $\log k_{12}$ is plotted versus $\Delta E_{1/2}$ for three organic solvent/water systems. The trend is consistent with Marcus theory,²⁶ where the rate increases with driving force at low driving force and decreases at high driving force. The reorganization energy is approximately equal to the average of the aqueous and organic self-exchange ET reorganization energies. As the organic redox couple is the same throughout, only the variation of the aqueous phase reorganization energy needs to be considered. The reorganization energy

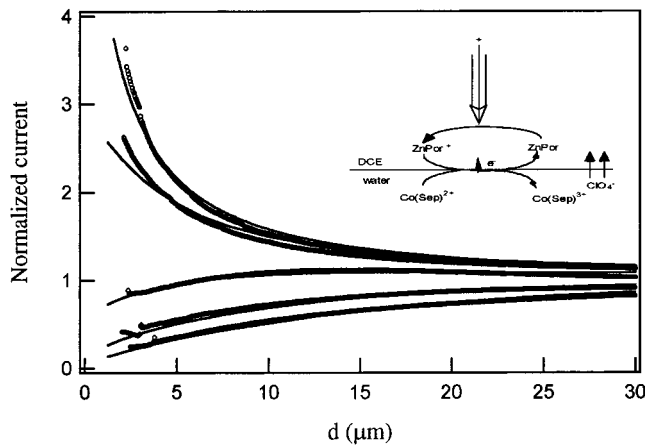


Figure 8. As in Figure 6 for the ET reaction between aqueous $Co(Sep)^{2+}$ and tip generated organic phase $ZnPor^+$ at the DCE/water interface where $K_r = 20, 10, 2,$ and 0.1 (top to bottom). Current was normalized with $i_{T,\infty} = 1.80$ nA. Solid lines show the simulated curves for a bimolecular rate constant of 4 $cm\ s^{-1}\ M^{-1}$.

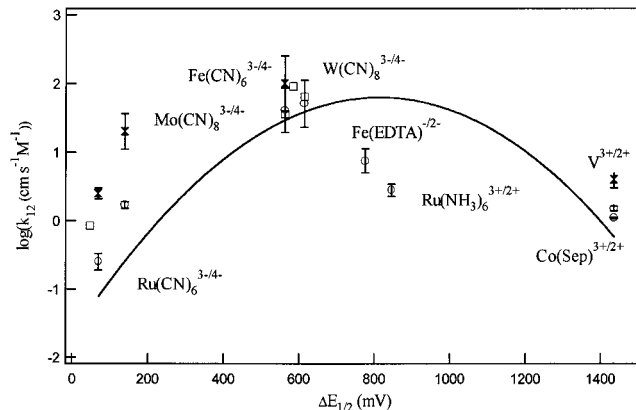


Figure 9. Dependence of the bimolecular rate constant, $\log(k_{12})$, on driving force, $\Delta E_{1/2}$, at the BN/water (O), benzene/water (\square), and DCE/water (filled \times) interfaces for heterogeneous ET between tip generated organic phase $ZnPor^+$ and aqueous $Ru(CN)_6^{4-}$, $Mo(CN)_8^{4-}$, $Fe(CN)_6^{4-}$, $W(CN)_8^{4-}$, $Fe(EDTA)^{2-}$, $Ru(NH_3)_6^{3+/2+}$, $V^{3+/2+}$, and $Co(Sep)^{3+/2+}$. Data for $Fe(EDTA)^{2-}$ at the BN/water interface are reprinted from ref 2. The solid line gives the Marcus prediction based on eq 1.

for cyano complexes is 0.32 eV,³³ while for $Ru(NH_3)_6^{3+/2+}$, $V^{3+/2+}$, and $Co(Sep)^{3+/2+}$, the values are 0.36,³⁴ 0.75,³⁴ and 0.62 eV,³⁴ respectively. The reorganization for $Fe(EDTA)^{2-}$ was not found. Neglecting the differences in reorganization energy between aqueous redox couples (most are essentially not significant), a general plot according to eq 1 with $\lambda \approx 0.85$ eV gives a trend consistent with the experimental data given in Figure 9.

It could be argued that the trend noted in Figure 9 reflects the variance of the self-exchange rate constant (k_{11}) of the chosen aqueous redox couples (eq 12 of ref 13) and not the parabolic dependence of rate on reaction free energy. Correlating k_{11} to the rate constant measured at the interfaces,¹⁶ ET involving $Ru(NH_3)_6^{3+}$ is interesting, as its self-exchange ET rate constant is known to be very high.³⁵ The k_{12} obtained for ET is given in Figure 9, and while the driving force for this reaction is greater than that for $Fe(CN)_6^{4-}$, the measured rate constant is smaller. This provides additional confirmation that the decrease noted at high overpotential is related to the free energy of the bimolecular reaction.

A recent report of ECL at an unmodified liquid/liquid interface¹⁸ is additional evidence for the existence of the Marcus inverted region. Previously, a solvent effect on the experimental

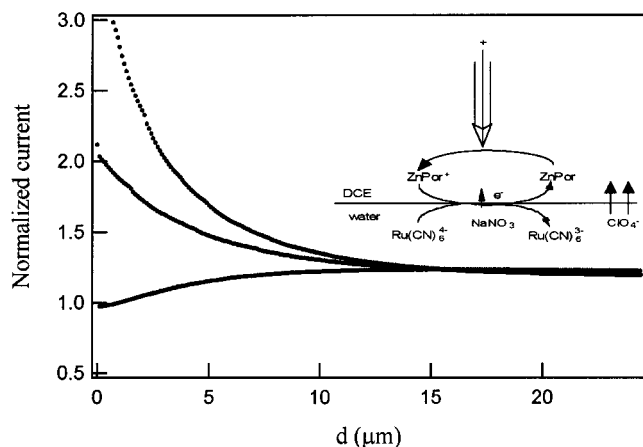


Figure 10. Approach curves illustrating the effect of increased aqueous phase ionic strength on the ET reaction between tip generated ZnPor^+ and aqueous $\text{Ru}(\text{CN})_6^{4-}$ at the DCE/water interface where aqueous $[\text{NaNO}_3] = 0, 0.1, \text{ and } 2 \text{ M}$ (top to bottom). Current was normalized with $i_{T,\infty} = 1.91 \text{ nA}$. The ClO_4^- concentrations in aqueous (10 mM NaClO_4) and organic phases (25 mM ThxAClO_4) were kept constant for the three curves.

rate constant was noted, and this was related to solvent relaxation and the solvent Pekar factor.¹⁰ In the results shown here, there is no obvious trend between solvents (DCE, BN, and benzene) and the rate constant.

3. Ionic Strength Dependence of the Observed Rate Constant. The effect of aqueous ionic strength was studied by the addition of NaNO_3 to the aqueous phase for the ET reaction between ZnPor^+ and $\text{Ru}(\text{CN})_6^{4-}$ at the DCE/water interface, where ClO_4^- was used as the potential determining ion. Approach curves obtained at various aqueous ionic strengths (0–2 M NaNO_3) are given in Figure 10. It is assumed that Na^+ and NO_3^- do not transfer readily across the interface.^{25,36} Clearly, as the NaNO_3 concentration increases, the approach curves begin to resemble those for negative feedback of a microelectrode tip approaching an insulating substrate; that is, the rate of ET drops off significantly. A similar observation was made by Zhang and Unwin,²⁰ who noted that the measured rate constant for ET between TCNQ^- and $\text{Fe}(\text{CN})_6^{3-}$ decreased as the concentration of Li_2SO_4 or NaCl added to the aqueous phase increased. This was attributed to a salting-out effect.³⁷ However, while Li_2SO_4 acts as a salting-out agent³⁸ at the water/DCE interface, NaCl does not;³⁹ the addition of high concentrations of NaCl does not induce a salting-out effect at the water/DCE interface. Rather, the available potential window at an externally polarized interface decreases as the salt concentration increases. The opposite effect is expected for an effective salting-out agent.³⁸ Thus, the decrease noted is unlikely to be due to the contribution of salting-out alone.

The effect of increased aqueous ionic strength on measured kinetic parameters is difficult to quantify, as it may depend on a wide variety of factors such as double layer effects,⁴⁰ specific or nonspecific adsorption,¹⁵ partitioning of ions,⁴¹ ET-ion transfer (IT), IT–IT coupling,^{42–44} salting-out, or a combination of these. All of these factors have the potential to decrease or increase the apparent rate constant. For example, adsorption of the base electrolyte ions at the interface could increase the distance between the reactants and decrease the apparent rate constant. This effect would become more pronounced as the concentration increases. Also, the addition of high concentrations of base electrolyte ions can also affect the driving force of the ET under study through ET–IT or IT–IT coupling. Even simple partitioning of base electrolyte ions may alter the interfacial

potential difference. Depending on the choice and concentration of supporting electrolyte ions, the potential established by the common ion may drive ion transfer of base electrolyte and ET. Such coupling has been previously considered,^{42–44} and estimation of the effect requires knowledge of the standard transfer potentials of all ions present in both phases. Note that in the previous cases (section 1 above), where the potential dependence of the rate constant was considered, the aqueous ionic strength was essentially constant for all concentration ratios of partitioning ions used. In this case, the effect of ionic strength is a background factor, which should affect the measured rate constant at each potential equally.

Rate constants measured by SECM studies are generally higher than those obtained at a conventionally polarized interface. While most SECM studies of ET to date have been carried out at relatively low ionic strengths, for interfaces under potentiostatic control, very high concentrations (>1 M) of Li_2SO_4 are typically added to prevent coupled IT of the ET products. The results obtained here and by Unwin's group indicate that the disparity in kinetic parameters may be related to the increased ionic strength.^{20,21}

Conclusions

From results presented in this report, we confirm that conventional theories of ET appear to be applicable to ITIES. While the detailed structure of the interface has not been resolved, the driving force between reactants can be varied through the applied interfacial potential difference. The dependence of rate on reaction free energy was demonstrated to be linear at low driving force (B–V region) and parabolic at high driving force (Marcus inverted region). High aqueous ionic strengths can have a pronounced effect on measured kinetic parameters, which should be taken into account in the interpretation of the data. SECM is a very useful technique for studying ET reactions at liquid/liquid interfaces.

Acknowledgment. The authors are indebted to Prof. P. R. Unwin for supplying the program for SECM curve fitting. Thanks to Drs. F. R. Frank Fan, Shigeru Amemiya, and Junfeng Zhou for their helpful discussions. The financial support for this research by the National Science Foundation (Grant CHE9870762) and the Robert A. Welch Foundation is gratefully acknowledged.

References and Notes

- (1) Amemiya, S.; Ding, Z.; Zhou, J.; Bard, A. J. *J. Electroanal. Chem.* **2000**, *483*, 7.
- (2) Barker, A. L.; Unwin, P. R.; Amemiya, S.; Zhou, J.; Bard, A. J. *J. Phys. Chem. B* **1999**, *103*, 7260.
- (3) Tsionsky, M.; Bard, A. J.; Mirkin, M. V. *J. Phys. Chem.* **1996**, *100*, 17881.
- (4) Zhang, J.; Slevin, C. J.; Unwin, P. R. *Chem. Commun.* **1999**, 1501.
- (5) Zhang, J.; Unwin, P. R. *Phys. Chem. Chem. Phys.* **2000**, *2*, 1267.
- (6) Shi, C.; Anson, F. C. *Electrochim. Acta* **1998**, *44*, 1301.
- (7) Shi, C.; Anson, F. C. *J. Phys. Chem. B* **1998**, *102*, 9850.
- (8) Shi, C.; Anson, F. C. *J. Phys. Chem. B* **1999**, *103*, 6283.
- (9) Ding, Z.; Fermin, D. J.; Brevet, P.-F.; Girault, H. H. *J. Electroanal. Chem.* **1998**, *458*, 139.
- (10) Liu, B.; Mirkin, M. V. *J. Am. Chem. Soc.* **1999**, *121*, 8352.
- (11) Marcus, R. A. *J. Phys. Chem.* **1990**, *94*, 1050.
- (12) Marcus, R. A. *J. Phys. Chem.* **1990**, *94*, 4152.
- (13) Marcus, R. A. *J. Phys. Chem.* **1991**, *95*, 2010.
- (14) Samec, Z.; Marecek, V.; Weber, J.; Homolka, D. *J. Electroanal. Chem. Interfacial Electrochem.* **1981**, *126*, 105.
- (15) Cheng, Y.; Schiffrin, D. J. *J. Chem. Soc., Faraday Trans.* **1993**, *89*, 199.
- (16) Wei, C.; Bard, A. J.; Mirkin, M. V. *J. Phys. Chem.* **1995**, *99*, 16033.
- (17) Tsionsky, M.; Bard, A. J.; Mirkin, M. V. *J. Am. Chem. Soc.* **1997**, *119*, 10785.
- (18) Zu, Y.; Fan, F.-R. F.; Bard, A. J. *J. Phys. Chem. B* **1999**, *103*, 6272.

- (19) Schmickler, W. *J. Electroanal. Chem.* **1997**, *429*, 123.
(20) Zhang, J.; Unwin, P. R. *J. Phys. Chem. B* **2000**, *104*, 2341.
(21) Zhang, J.; Barker, A. L.; Unwin, P. R. *J. Electroanal. Chem.* **2000**, *483*, 95.
(22) Martin, E. L. In *Organic Reactions*; Bachmann, W. E., Johnson, J. R., Fieser, L. F., Snyder, H. R., Eds.; John Wiley & Sons: New York, 1942; Vol. 1, p 163.
(23) Bard, A. J.; Fan, F. R. F.; Mirkin, M. V. In *Electroanalytical Chemistry*; Bard, A. J., Ed.; Marcel Dekker: New York, 1994; Vol. 18, p 243.
(24) Shao, Y.; Mirkin, M. V. *J. Electroanal. Chem.* **1997**, *439*, 137.
(25) Girault, H. H.; Schiffrin, D. J. In *Electroanalytical Chemistry*; Bard, A. J., Ed.; Marcel Dekker: New York, 1989; Vol. 15, p 1.
(26) Marcus, R. A. *J. Chem. Phys.* **1965**, *43*, 679.
(27) Shao, Y.; Mirkin, M. V. *J. Phys. Chem. B* **1998**, *102*, 9915.
(28) Mirkin, M. V. In *Scanning Electrochemical Microscopy*; Bard, A. J., Mirkin, M. V., Eds.; Marcel Dekker: New York, in press; Chapter 4.
(29) Ding, Z.; Wellington, R. G.; Brevet, P. F.; Girault, H. H. *J. Phys. Chem.* **1996**, *100*, 10658.
(30) Solomon, T.; Bard, A. J. *J. Phys. Chem.* **1995**, *99*, 17487.
(31) Bard, A. J.; Faulkner, L. R. *Electrochemical Methods*; Wiley: New York, 1980.
(32) Girault, H. H.; Schiffrin, D. J. *J. Electroanal. Chem.* **1988**, *244*, 15.
(33) Crnogorac, M. M.; Kostic, N. M. *Inorg. Chem.* **2000**, *39*, 5028.
(34) Sutin, N.; Weaver, M. J.; Yee, E. L. *Inorg. Chem.* **1980**, *19*, 1096.
(35) Brown, G. M.; Sutin, N. *J. Am. Chem. Soc.* **1979**, *101*, 883.
(36) Hundhammer, B.; Solomon, T. *J. Electroanal. Chem.* **1983**, *157*, 19.
(37) Geblewicz, G.; Schiffrin, D. J. *J. Electroanal. Chem.* **1988**, *244*, 27.
(38) Geblewicz, G.; Kontturi, A. K.; Kontturi, K.; Schiffrin, D. J. *J. Electroanal. Chem. Interfacial Electrochem.* **1987**, *217*, 261.
(39) Kontturi, A.-K.; Kontturi, K.; Murtomaeki, L.; Quinn, B. *Acta Chem. Scand.* **1996**, *50*, 640.
(40) Kakiuchi, T.; Senda, M. *Bull. Chem. Soc. Jpn.* **1983**, *56*, 1753.
(41) Kakiuchi, T. In *Liquid-Liquid Interfaces*; Volkov, A. G., Deamer, D. W., Eds.; CRC Press: Boca Raton, FL, 1996; p 1.
(42) Kakiuchi, T. *Electrochim. Acta* **1995**, *40*, 2999.
(43) Kakiuchi, T.; Takaishi, T. *Proc. Electrochem. Soc.* **1997**, *97-19*, 538.
(44) Shafer, H. O.; Derback, T. L.; Koval, C. A. *J. Phys. Chem. B* **2000**, *104*, 1025.